Inorganic Chemistry

Article

pubs.acs.org/IC

Zn^{2+} Responsive Bimodal Magnetic Resonance Imaging and Fluorescent Imaging Probe Based on a Gadolinium(III) Complex

Jian Luo, Wei-Sheng Li, Peng Xu, Li-Yi Zhang, and Zhong-Ning Chen*

State Key Laboratory of Structural Chemistry, Fujian Institute of Research on the Structure of Matter, Chinese Academy of Sciences, 155 Yangqiao Road West, Fuzhou 350002, China

Supporting Information

ABSTRACT: A Zn^{2+}-responsive bimodal magnetic resonance imaging (MRI) and luminescence imaging probe GdL was synthesized. The relaxivity and luminescence properties were examined. In the presence of 0.5 equiv of Zn^{2+}, the longitudinal relaxivity is increased from 3.8 mM^{-1} s^{-1} to 5.9 mM^{-1} s^{-1} at 23 MHz and 25 °C with 55% enhancement, whereas the fluorescence exhibits a 7-fold increase. The Zn^{2+} responsive imaging probe shows favorable selectivity and tolerance over a variety of biologically relevant anions and metal ions in physiological pH range for both relaxivity and luminescence. In vitro phantom images and confocal fluorescence images in living cells show that the bimodal Zn^{2+} probe can effectively enhance T_1-weighted imaging contrast and luminescence imaging effect through Zn^{2+} coordination with excellent cellmembrane permeability and biocompatibility. Spectral and electrospray ionization mass spectrometry (ESI-MS) studies indicate that two different Zn^{2+}-bound species, $(GdL)_2Zn$ and GdLZn, are formed when 0.5 and 1 equiv of Zn^{2+} are bound to GdL complex, respectively. Crystal structural determination and dysprosium-induced ^{17}O NMR shift (DIS) experiment demonstrate that the increased molecular weight and the improved molecular rigidity upon complexation of Zn^{2+} with GdL is the primary factor for relaxivity enhancement. Significant enhancement of the luminescence is due to a heavy atom effect and much increased molecular rigidity upon Zn^{2+} binding to 8-sulfonamidoquinoline chromophore.

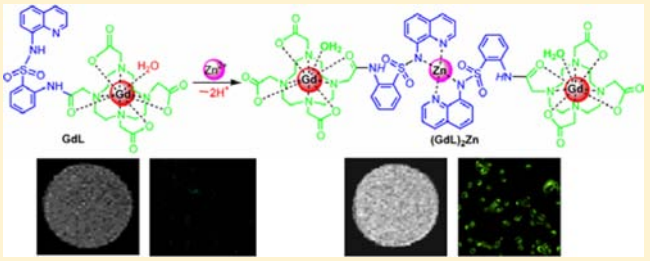

INTRODUCTION

Multiple imaging techniques have been widely applied in clinical diagnostics although none of them could provide comprehensive information of the human body each because of their own limitations.[1] Recently, the development of bimodal or multimodal imaging agents with the combination of two or more molecular imaging techniques has been receiving more and more attention.[1b] Luminescence imaging and magnetic resonance imaging (MRI) are both powerful approaches in disease diagnostic, and in fact they are complementary analytical techniques. As a sensitive, specific, and fast response analytical method, luminescence imaging is suitable for generating high-resolution images but could not penetrate in thick tissues owing to lack of optical transparency.[2] In contrast, MRI is a safe, noninvasive, and nonradiative technique that is perfect for providing whole body images, but its spatial resolution is only in the 0.1 mm range.[2b,3] When luminescence imaging and MRI are synchronously used, much more complete information regarding tissue and organs in the human body can thus be obtained.

Several bimodal MRI and luminescence imaging agents based on gadolinium(III) systems or magnetic nanoparticles (NPs) have been reported in recent years.[1b,2b,4] Some GdDO3A-based smart MRI contrast agents with selective response to specific metal ions or anions in the human body have been also developed.[5] Nevertheless, bimodal MRI and luminescence imaging agents that respond to specific metal ions or chemical species in living biological systems have been less explored except for one Cu^{2+}-selective GdDO3A-based MRI contrast agent that exhibits luminescence turn-off response.[6] It represents a significant challenge for synthetic chemists to achieve responsive bimodal MRI/luminescence imaging probes that exhibit simultaneous turn-on effect in both luminescence and relaxivity in response to a specific metal ion or a biologically relevant substance.

According to the Solomon−Bloembergen−Morgan equation,[7] the factors that contribute to the relaxivity for a MRI contrast agent include the number of inner-sphere water molecules (q), the rotational tumbling time (τ_R), and the residence lifetime of inner-sphere water molecules (τ_m).[3,5a,8] To design a responsive dual-mode contrast agent with turn-on effect in both luminescence and relaxivity, it is necessary to increase the number of inner-sphere water molecules (q), increase molecular weight, or improve molecular rigidity of the contrast agents upon metal ion binding to chromophores with switch-on luminescence.

Since quinoline-based compounds are ideal probes for Zn^{2+} because of their high selectivity, low toxicity, cell permeability, and relatively convenient synthetic procedure and functional-

Received: June 20, 2012
Published: August 10, 2012

dx.doi.org/10.1021/ic301308z | Inorg. Chem. 2012, 51, 9508−9516

Scheme 1. Synthetic Routes to GdL[a]

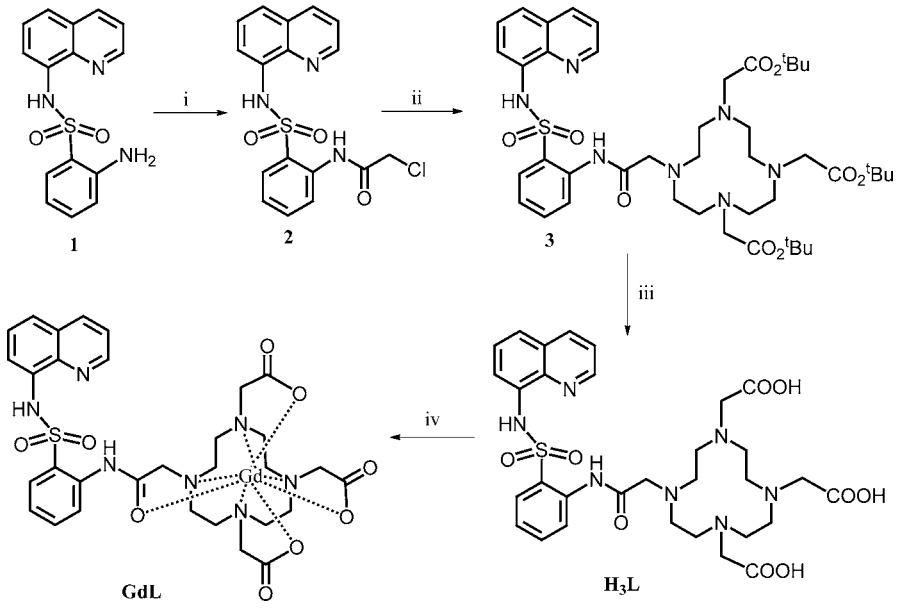

[a](i) Chloroacetyl chloride, triethylamine, rt, 4 h; (ii) tris-*tert*-butyl-DO3A, K_2CO_3, CH_3CN, 70°C, 1 d; (iii) TFA/CH_2Cl_2 (1: 1), rt, 1 d; (iv) $GdCl_3 \cdot 6H_2O$, water, pH = 7.0, rt, 1 d.

ization,[9] 8-sulfonamidoquinoline chromophore is elaborately introduced to a Gd-DO3A moiety so that Zn^{2+}-responsive MRI and luminescence imaging agent GdL (Scheme 1) was thus accessed with significant enhancement in both relaxivity and luminescence. This Zn^{2+}-responsive bimodal imaging probe shows favorable selectivity and tolerance over a variety of biologically relevant anions and metal ions in physiological pH range. Effectively improved T_1-weighted imaging contrast and strikingly enhanced luminescence imaging effect together with good cell membrane permeability and biocompatibility were demonstrated through in vitro phantom images and confocal fluorescence images in living cells.

RESULTS AND DISCUSSION

Synthetic routes to complex GdL are depicted in Scheme 1. Reaction of **1** with 1.2 equiv of chloroacetyl chloride in the presence of triethylamine gave **2** in 70% yield. Compound **3** was prepared by the reaction of **2** and tris-*tert*-butyl-DO3A in the presence of K_2CO_3 in 53% yield. Ligand H_3L in 92% yield was then accessed through removal of protected tris-*tert*-butylester in trifluoroacetic acid (TFA) and CH_2Cl_2 (v/v = 1:1). Addition of equimolar $GdCl_3 \cdot 6H_2O$ to an aqueous solution of H_3L by maintaining pH = 7.0 using 1 M NaOH solution thus afforded complex GdL as a white powder.

The longitudinal relaxivity r_1 of GdL was investigated by a 23 MHz NMR Analyzing & Imaging system at 25 °C in 100 mM HEPES buffer solution at pH = 7.2. The r_1 of GdL was estimated as 3.8 mM^{-1} s^{-1}, which was gradually increased with the addition of Zn^{2+}. Upon addition of 0.5 equiv of Zn^{2+}, the r_1 was increased to 5.9 mM^{-1} s^{-1} with 55% enhancement. When 1 equiv of Zn^{2+} was added, the r_1 was measured as 5.2 mM^{-1} s^{-1}. Nevertheless, further change of r_1 value was not observed by addition of more than 1 equiv of Zn^{2+} (Figure 1). It is known that the parent gadolinium(III) complex of 1,4,7,10-tetraazadodecanetetraacetic acid (Gd-DOTA) exhibited a relaxivity of 3.9 mM^{-1} s^{-1} when it was recorded on a 400 MHz NMR spectrometer at 25 °C.[10] T_1 measurements of GdL were also performed at 400 MHz and 25 °C, and the r_1 value of GdL was estimated as 4.0 mM^{-1} s^{-1} in this condition. Although GdL affords a comparable relaxivity with parent Gd-DOTA at high field (9.4 T), it exhibits significantly Zn^{2+}-responsive relaxivity change with 55% relaxivity enhancement (5.9 mM^{-1} s^{-1}) at low field (0.5 T). The overall variation in relaxivity upon addition of Zn^{2+} is sufficiently sensitive for specific detection of Zn^{2+} in physiological conditions. As shown in Figure 1, T_1-weighted imaging contrast of GdL was strikingly enhanced upon addition of 0.5 or 1 equiv of Zn^{2+}.

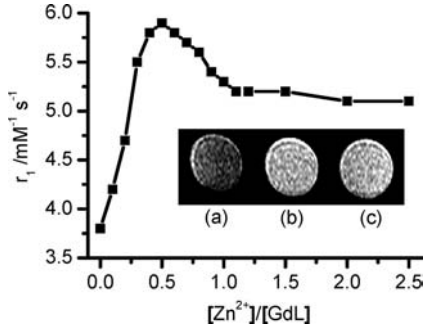

Figure 1. Relaxivity titration of GdL with Zn^{2+} in 100 mM HEPES buffer at pH = 7.2. All the measurements were performed at 23 MHz and 25 °C. The inner picture of T_1-weighted phantom MR images of 0.5 mM GdL in the absence (a) or presence of (b) 0.5 equiv of Zn^{2+} and (c) 1 equiv of Zn^{2+}.

To detect selectivity and tolerance of GdL in response to Zn^{2+}, the relaxivity measurement was carried out in the presence of other biological metal ions (Figure 2). The r_1 of GdL was almost unchanged by the addition of 0.5 equiv of Ca^{2+} (3.9 mM^{-1} s^{-1}), Mg^{2+} (3.9 mM^{-1} s^{-1}), Fe^{2+} (3.8 mM^{-1} s^{-1}), or Fe^{3+} (3.7 mM^{-1} s^{-1}). The interference experiments were carried out in the same conditions by the addition of 0.5 equiv of Zn^{2+} and 0.5 equiv of an interfering metal ion. As depicted in Figure 2, Zn^{2+}-enhanced relaxivity of GdL was little influenced by other biological metal ions such as Ca^{2+} (5.9 mM^{-1} s^{-1}),

dx.doi.org/10.1021/ic301308z | Inorg. Chem. 2012, 51, 9508−9516

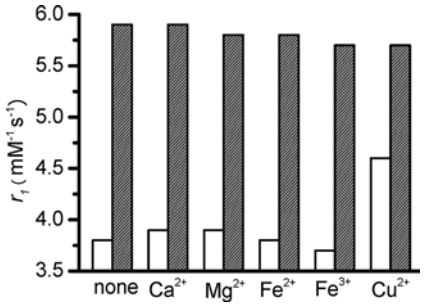

Figure 2. Relaxivity of GdL at 23 MHz in the presence of various metal ions at 25 °C. Blank bars represent the relaxivity upon addition of 0.5 equiv of appropriate metal ion to the solutions of GdL. Shadow bars represent the relaxivity upon addition of 0.5 equiv of Zn^{2+} together with 0.5 equiv of another interfering metal ion to the solutions of GdL. All solutions were prepared in 100 mM HEPES buffer at pH = 7.2.

Mg^{2+} (5.8 mM^{-1} s^{-1}), Cu^{2+} (5.7 mM^{-1} s^{-1}), Fe^{2+} (5.8 mM^{-1} s^{-1}), and Fe^{3+} (5.7 mM^{-1} s^{-1}). Thus, complex GdL exhibits highly selectivity in response to Zn^{2+} with remarkable relaxivity enhancement which is almost undisturbed by other biological metal ions. Although GdL displays a little relaxivity enhancement in response to 0.5 equiv of Cu^{2+} (4.6 mM^{-1} s^{-1}), the interference of Cu^{2+} is still limited considering that the content of Cu^{2+} is only about 1/20 of Zn^{2+} in the human body.[11] Furthermore, the calculated stability constant of GdLCu (4.2×10^4 M^{-1}) is much smaller than that of $(GdL)_2Zn$ (4.2×10^{11} M^{-2}) or GdLZn (2.1×10^6 M^{-2}) species (vide infra), suggesting that the binding capability of GdL to Zn^{2+} is much larger than that to Cu^{2+}. As indicated in Figure 3, the relaxivity of GdL was increased from 3.6 mM^{-1} s^{-1} to 5.0 mM^{-1} s^{-1} in response to 0.5 equiv of Zn^{2+} even if the measurement was carried out in a simulated biological solution system that contains 5 mM K^+, 2 mM Ca^{2+}, 0.7 mM Mg^{2+}, 0.5 mM Fe^{2+}, 0.5 mM Fe^{3+}, and 0.1 mM Cu^{2+} as well as a series of biological anions (vide infra).

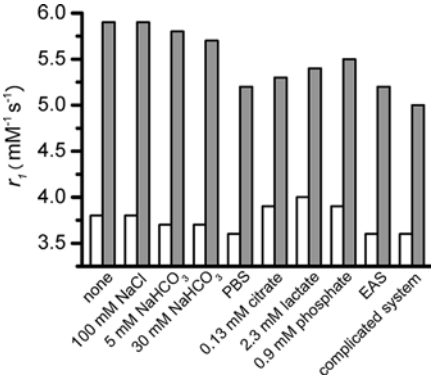

Figure 3. Relaxivity response of GdL to 0.5 equiv of Zn^{2+} at 23 MHz in the presence of biologically relevant anions. Blank bars represent the relaxivity of GdL in the presence of corresponding anions. Shadow bars represent the relaxivity upon addition of 0.5 equiv of Zn^{2+} to GdL in presence of corresponding anions. All measurements were performed in 100 mM HEPES buffer, pH = 7.2 except for PBS, EAS, and the complicated system. The relaxivity measurement with PBS was acquired under similar conditions using PBS, pH = 7.4. EAS contains 30 mM $NaHCO_3$, 100 mM NaCl, 0.9 mM KH_2PO_4, 2.3 mM sodium lactate, and 0.13 mM sodium citrate, pH = 7.0. A complicated solution system contains all the anions in ESA as well as 5 mM KCl, 2 mM $CaCl_2$, 0.7 mM $MgCl_2$, 0.5 mM $FeCl_2$, 0.5 mM $FeCl_3$, and 0.1 mM $CuCl_2$, pH = 7.0.

There are various anions that exist in human body, and some of them display high concentration, which may affect the relaxivity of Gd-based contrast agents.[12] To determine the tolerance of this Zn^{2+}-responsive MRI system to various biological anions, Zn^{2+}-responsive relaxivity changes of GdL were investigated in the presence of a variety of biological anions at physiologically relevant concentrations. As shown in Figure 3, the influence by most of the anions is negligible except for citrate and lactate which induce a little less relaxivity enhancement of GdL in response to 0.5 equiv of Zn^{2+}. Nevertheless, when a simulated extracellular anion solution (EAS) containing 30 mM $NaHCO_3$, 100 mM NaCl, 0.9 mM KH_2PO_4, 2.3 mM sodium lactate, and 0.13 mM sodium citrate (pH = 7.0)[13] was used, GdL displayed 45% enhancement of the relaxivity in response to 0.5 equiv of Zn^{2+}. Consequently, GdL displays a satisfactory tolerance to various biological anions and metal ions.

Complex GdL is also a selective luminescence sensor for Zn^{2+}. Luminescence studies were carried out at 25 °C in a 100 mM HEPES buffer solution at pH = 7.2. Figure 4 depicts the emission spectral changes of GdL in the presence of various metal ions. Although the 8-sulfonamidoquinoline chromophore of GdL exhibited weak emission centered at 496 nm, addition of 0.5 equiv of Zn^{2+} resulted in 7-fold luminescence enhancement and a distinct red-shift to 503 nm because of an internal charge transfer process from 8-sulfonamidoquinoline chromophore to Zn^{2+}.[9d] When 1 equiv of Zn^{2+} was added, the emission spectrum was red-shifted to 530 nm with 5.5-fold luminescence enhancement relative to GdL. As shown in Figure 4 (inset), bright green and yellow-green emitting was observed when 0.5 and 1.0 equiv of Zn^{2+} was added to a 50 μM solution of GdL with the emission centered at 503 and 530 nm, respectively. Interference (Figure 5) experiments revealed that distinct luminescence changes were not observed upon addition of 0.5 equiv of biological metal ion to the solution of GdL except that Cu^{2+} significantly quenched the emission. Although both Fe^{3+} and Cu^{2+} are paramagnetic and redox-active, it is likely that complexation of Cu^{2+} to GdL induces quenching of the emission whereas Fe^{3+} is existent in free ion without binding to GdL.

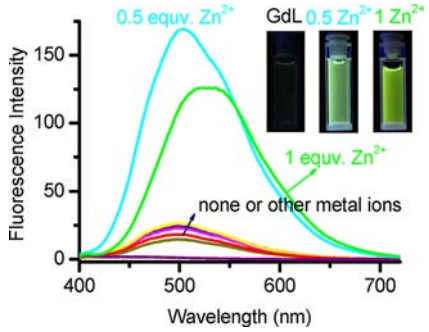

Figure 4. Fluorescence spectra of GdL (20 μM) in the presence of 0.5 or 1 equiv of Zn^{2+}, and 1 equiv of K^+, Na^+, Ca^{2+}, Mg^{2+}, Fe^{2+}, Fe^{3+}, and Cu^{2+} in 100 mM HEPES buffer solutions at 25 °C, pH = 7.2 (λ_{ex} = 360 nm). Inset luminescence photographs were taken from 50 μM GdL solutions in the absence and presence of 0.5 or 1 equiv of of Zn^{2+} under UV light irradiation at 365 nm.

dx.doi.org/10.1021/ic301308z | Inorg. Chem. 2012, 51, 9508−9516

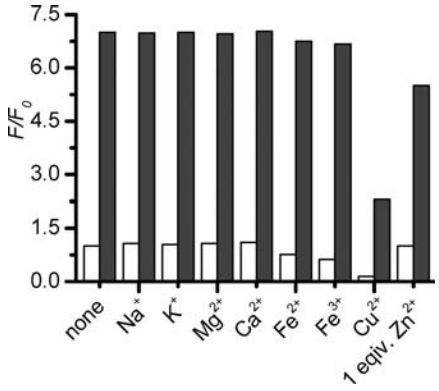

Figure 5. Fluorescence (λ_{ex} = 360 nm) intensity of GdL (20 μM) in the presence of 0.5 equiv of biological metal ions (blank bars), or 0.5 equiv of Zn^{2+} together with 0.5 equiv of an interfering metal ion (shadow bars). The last two bars represent the fluorescence intensity of GdL (20 μM) in the absence (blank bar) and presence (shadow bar) of 1 equiv of Zn^{2+}.

Zn^{2+}-responsive luminescence imaging of GdL in breast cancer cell line MDA-MB-231 was investigated through confocal luminescence microscopy. Incubation of MDA-MB-231 cells with 20 μM GdL in PBS buffer for 30 min at 37 °C gave a very weak intracellular luminescence (Figure 6a). When the cells were subsequently incubated with Zn^{2+} (30 μM) at 37 °C for 20 min, the yellow-green luminescence became much brighter which was clearly observable to the naked-eye (Figure 6d). Bright-field measurements (Figure 6b and 6e) indicated that the cells were viable throughout the imaging experiments upon treatment with GdL and Zn^{2+}, respectively. It appears that complex GdL can be ingested harmlessly by living cells. As depicted in Figure 6f, the luminescence signals of GdL-Zn species were mainly localized at the cytoplasm, implying good cell membrane permeability and an intracellular distribution of GdL-Zn species.

The emission spectral changes were monitored by titration of GdL with Zn^{2+} in 100 mM HEPES buffer solutions at pH = 7.2 (Figure 7). The luminescence was first progressively enhanced

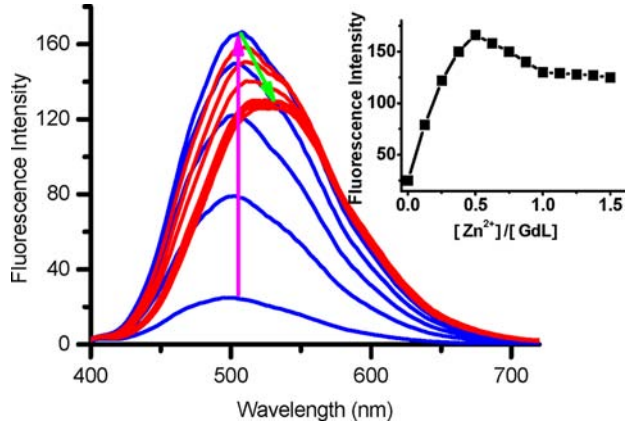

Figure 7. Emission spectral changes of GdL (20 μM) upon addition of Zn^{2+} ([Zn^{2+}] = 0, 2.5, 5, 7.5, 10, 12.5, 15, 17.5, 20, 22.5, 25, 27.5, and 30 μM) in 100 mM HEPES buffer solutions at 25 °C, pH = 7.2 (λ_{ex} = 360 nm).

to reach a maximum at 503 nm when 0.5 equiv of Zn^{2+} was added. Further addition of more than 0.5 equiv of Zn^{2+} induced a red-shift of the emission at 503 to 530 nm with a little reduced luminescence intensity. The two-step emission spectral changes thus suggest the formation of two types of Zn^{2+}-bound species depending on the amount of Zn^{2+} added. As revealed by electrospray ionization mass spectrometry (ESI-MS) studies, when 0.5 equiv of Zn^{2+} was added, the base peak at 1741.5 corresponded to the molecular ion peak of $(GdL)_2Zn$ (Supporting Information, Figure S6) through complexation of one Zn^{2+} with two GdL moieties. When 1 equiv of Zn^{2+} was used, the observed base peak at 938.0 ($[M+2H_2O-H^+]^-$) implied the formation of species GdLZn (Supporting

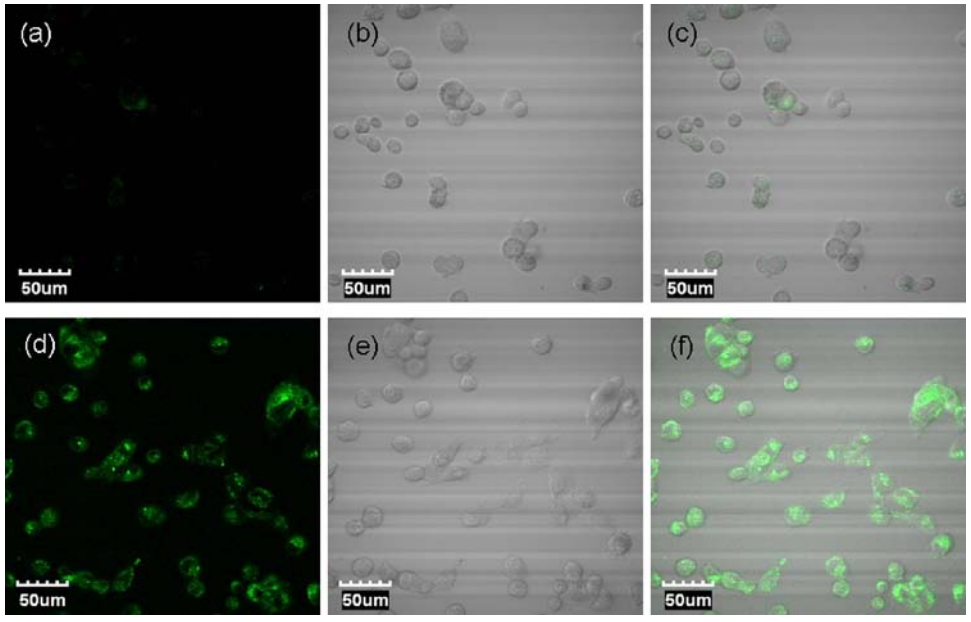

Figure 6. Confocal fluorescence images in MDA-MB-231cells. (a) Cells incubated with 20 μM GdL in PBS buffer for 30 min; (b) Bright-field image of (a); (c) Overlay image of (a) and (b); (d) Cells incubated first with 20 μM GdL in PBS buffer for 30 min, and then incubated with 30 μM Zn^{2+} for 20 min; (e) Bright-field image of (d); (f) Overlay image of (d) and (e).

dx.doi.org/10.1021/ic301308z | Inorg. Chem. 2012, 51, 9508−9516

Information, Figure S7) with a 1:1 ratio between Zn^{2+} and GdL. The stability constants of $(GdL)_2Zn$ (k_a) and GdLZn (k_b) species defined in eqs 1−3 were determined as 4.2×10^{11} M^{-2} and 2.1×10^6 M^{-1}, respectively.

$$2GdL + Zn^{2+} \overset{k_a}{\rightleftharpoons} (GdL)_2Zn$$

$$k_a = \frac{[(GDL)_2Zn]}{[GdL]^2[Zn^{2+}]} \quad (1)$$

$$GdL + Zn^{2+} \overset{k_b}{\rightleftharpoons} GdLZn$$

$$k_b = \frac{[GdLZn]}{[GdL][Zn^{2+}]} \quad (2)$$

$$GdL + Cu^{2+} \overset{k_{Cu}}{\rightleftharpoons} GdLCu$$

$$k_{Cu} = \frac{[GdLCu]}{[GdL][Cu^{2+}]} \quad (3)$$

The UV−vis spectral changes by titration of GdL with Zn^{2+} revealed that a new absorption band at 360 nm (Supporting Information, Figure S2) which reached the maximum upon addition of 1 equiv of Zn^{2+}. Similarly, titration of GdL with Cu^{2+} resulted in a new absorption band centered at 370 nm (Supporting Information, Figure S3), which was gradually increased to the maximum upon addition of 1 equiv of Cu^{2+}. The calculated stability constant of GdLCu (k_{Cu}) as defined in eq 3 is 4.2×10^4 M^{-1}. The pH-dependent Zn^{2+}-responsive fluorescence changes (Supporting Information, Figure S4) of GdL suggested that the fluorescence of $(GdL)_2Zn$ and GdLZn complexes reached their maxima at pH = 6 and 5.5, respectively. At pH = 7.2 in physiological condition, the fluorescence exhibits 7- and 5.5-fold enhancement upon formation of $(GdL)_2Zn$ and GdLZn species, respectively.

The structure of neutral complex $GdLZn(H_2O)_3 \cdot 5H_2O$ was successfully determined by X-ray crystallography. Because of the difficulty in crystallization, only a limited number of Gd-DO3A complexes have been characterized by single crystal X-ray diffraction.[2b,3b,14] As depicted in Figure 8, the Gd^{3+} is nine-coordinated to adopt a monocapped square antiprismatic geometry with eight apexes occupied by four amine N, three carboxylate O, and one amide O donors whereas the capped site is occupied by a H_2O molecule. The $Gd-OH_2$ length (2.500(3) Å) is much longer than other four Gd−O bonds (2.359(2)−2.382(3) Å), and also a little longer than that found in $Na[Gd(DOTA)(H_2O)]$ (2.458 Å).[15] The Zn^{2+} is five-coordinated to give a distorted trigonal bipyramid, in which the trigonal plane is composed of amide N (N5), quinoline N (N7), and one coordinated H_2O (O12) whereas two pyramidal apexes are occupied by sulfamide N (N6) and another coordination H_2O (O11).

Dysprosium-induced ^{17}O NMR shift (DIS) experimental studies on DyL and its Zn^{2+}-bound complex $(DyL)_2Zn$ were performed so that the number of coordination hydration (q) in aqueous solution was determined, respectively. The corresponding DIS data for Zn^{2+}-bound DyLZn species, however, was not obtained because of its solubility limitation in a high concentration. Calibrations with standard DIS plots for $DyCl_3$ (q = 9) to determine q values were performed by Peters's method.[15] As depicted in Figure 9, a plot of DIS versus $DyCl_3$ concentration in HEPES buffer solution revealed a slope of 332 ppm/M, corresponding to 37 ppm/M shift per coordination

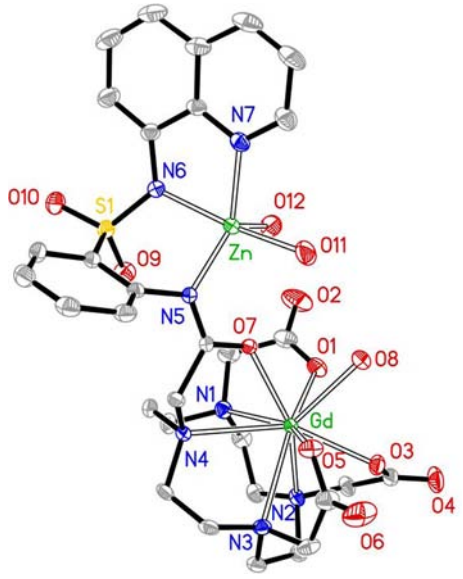

Figure 8. ORTEP drawing of neutral complex GdLZn with atom-labeling scheme showing 30% thermal ellipsoid.

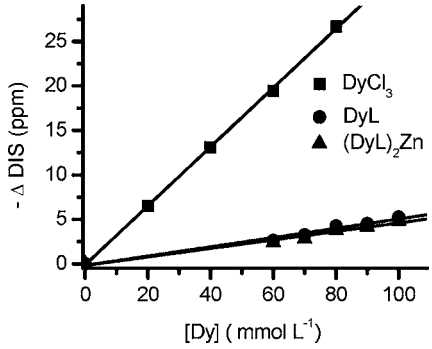

Figure 9. Plots of DIS of the ^{17}O NMR signals of H_2O (−Δ, ppm) vs [Dy] for $DyCl_3$ (■), DyL (●), and $(DyL)_2Zn$ (▲). The ^{17}O NMR spectra were recorded at room temperature in 100 mM HEPES buffer solutions containing 20% D_2O, pH = 7.2.

water molecule. The measured ^{17}O NMR shift for DyL was 52 ppm/M, corresponding to q = 1.4. When 0.5 equiv of Zn^{2+} was added to the solution of DyL, the corresponding DIS was measured as 48 ppm/M, corresponding to q = 1.3 in complex $(DyL)_2Zn$. The ^{17}O NMR experimental studies thus suggest that one coordination water remains unchanged upon complexation of two DyL with one Zn^{2+} to form $(DyL)_2Zn$. This coincides is well with that in the heteronuclear complex GdLZn, in which one H_2O molecule (q = 1) bound to Gd^{3+} was unambiguously determined by X-ray crystallography. Consequently, Zn^{2+}-triggered relaxivity enhancement in this system is not because of the changes in inner-sphere coordination water molecules (q) upon complexation of GdL with Zn^{2+}.

To make a mechanistic elucidation of Zn^{2+}-enhanced relaxivity and luminescence, a proposed schematic diagram is depicted in Scheme 2, showing formation of heterotrinuclear array $(GdL)_2Zn$ through loss of a sulfamide proton as well as heterobinuclear array GdLZn through further loss of an amide proton upon GdL binding to 0.5 and 1 equiv of Zn^{2+}, respectively. The Gd^{3+} in GdL is nine-coordinated, in which eight apexes are occupied by N and O donors from L, whereas another site is bonded to one H_2O molecule with q = 1. When

dx.doi.org/10.1021/ic301308z | Inorg. Chem. 2012, 51, 9508−9516

Scheme 2. Schematic Binding Mode of GdL Bound to Zn^{2+}

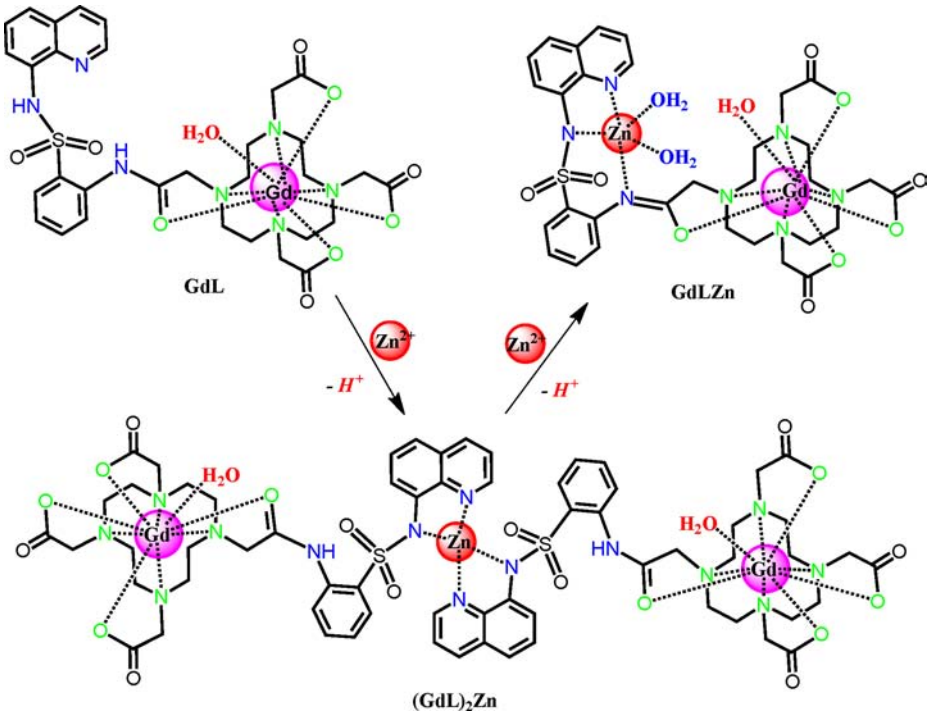

one Zn^{2+} is bound to two GdL moieties through monoanionic *N*,*N*-bidentate 8-sulfonamidoquinoline moieties, heterotrinuclear complex $(GdL)_2Zn$ is formed in a 1:2 binding stoichiometry between GdL and Zn^{2+}, in which each Gd^{3+} remains in coordination to one H_2O. The relaxivity enhancement from 3.8 to 5.9 mM^{-1} s^{-1} is ascribed to an increased molecular weight of $(GdL)_2Zn$ relative to the precursor GdL, thus inducing a longer rotational tumbling time. The luminescence is significantly enhanced because of a heavy atom effect upon Zn^{2+} binding to 8-sulfonamidoquinoline chromophore. There exist intermolecular hydrogen bonds between pyridyl N atom and sulfanilamide of 8-sulfonamidoquinoline chromophore in free precursor GdL, which results in photoinduced electron transfer and nonradiative deactivation.[9d] When 8-sulfonamidoquinoline is coordinated to Zn^{2+}, the electron-transfer deactivation is largely prohibited upon formation of Zn^{2+}-coordinated system with more extended π-conjugation so that the luminescence exhibits significant enhancement with a distinct red-shift from 496 to 503 nm.

When Zn^{2+} is bound to GdL with formation of GdLZn in a 1:1 ratio between GdL and Zn^{2+}, the dianionic *N*-(quinolin-8-yl)-2-acetamino-benzenesulfonamide moiety acts as a terdentate ligand to chelate Zn^{2+} through sulfamide N, quinoline N, and amide N donors (Scheme 2) so that the luminescence is red-shifted to 530 nm because of better π-conjugation in GdLZn than that in $(GdL)_2Zn$. Even if the molecular weight of GdLZn (903) is not remarkably increased compared with GdL (840), free rotation and wobble at amide C−N, C(phenyl)−N(amide), sulfamide N−S, and S−C(phenyl) bonds of *N*-(quinolin-8-yl)-2-acetamino-benzenesulfonamide moiety are totally prohibited so that the molecular structure of GdLZn is much more constrained to afford a significantly improved rigidity compared with GdL, which induce a longer rotational tumbling time. This makes GdLZn have a higher relaxivity value than GdL. Nevertheless, the molecular weight of GdLZn is much smaller than that of $(GdL)_2Zn$ (1742) so that the longitudinal relaxivity of GdLZn (5.2 mM^{-1} s^{-1}) is a little lower than that of $(GdL)_2Zn$ (5.9 mM^{-1} s^{-1}), but still much higher than that of GdL (3.8 mM^{-1} s^{-1}). Therefore, Zn^{2+}-responsive relaxivity enhancement for GdL results mostly from the increased molecular weight for $(GdL)_2Zn$ and improved molecular rigidity[3c,4d,16] for GdLZn when Zn^{2+} is chelated to 8-sulfonamidoquinoline chromophore. Overall, the increased molecular weight is a more important factor than other factors for Zn^{2+}-coordination triggered relaxivity enhancement in this system.

CONCLUSION

A Zn^{2+}-responsive bimodal MRI and fluorescent imaging probe was elaborately designed. It exhibits obvious Zn^{2+}-responsive relaxivity enhancement with improved signal contrast as well as significant turn-on luminescence. The relaxivity enhancement originates mostly from the increase in molecular weight as well as the improvement in molecular rigidity through Zn^{2+} coordination. Significantly enhanced luminescence is ascribed to a heavy atom effect and much increased molecular rigidity upon Zn^{2+} binding to 8-sulfonamidoquinoline chromophore. The sensitivity and tolerance of this Zn^{2+}-responsive luminescence and MRI bimodal sensor toward other common biological metal ions and anions is satisfactory. Furthermore, this Zn^{2+}-responsive bimodal sensor displays good biocompatibility and cell membrane permeability.

EXPERIMENTAL SECTION

General Procedures and Materials. All chemicals were reagent grade and purchased from commercial sources. All reactions were carried out under a dry argon atmosphere by using Schlenk techniques and vacuum line systems unless otherwise specified. The solvents were dried, distilled, and degassed prior to use. The *N*-(quinolin-8-yl)-2-amino-benzenesulfonamide (**1**) was synthesized by Landry's method.[17] The tris-*tert*-butyl-DO3A (**3**) was modified by Finn's method.[18]

***N*-(Quinolin-8-yl)-2-(2-chloroacetyl)-amino-benzenesulfonamide (2).** To a CH_2Cl_2 (25 mL) solution of **1** (0.5 g, 1.7 mmol) and

dx.doi.org/10.1021/ic301308z | *Inorg. Chem.* 2012, 51, 9508−9516

triethylamine (0.202 g, 2.0 mmol) cooled in an ice bath was added dropwise a CH_2Cl_2 (5 mL) solution of chloroacetyl chloride (0.226 g, 2.0 mmol) with stirring. After 4 h stirring at room temperature, the reaction mixture was washed with 1 M $NaHCO_3$ aqueous (30 mL) solution and brine (30 mL). The organic layer was dried over Na_2SO_4 and concentrated. The product was purified by chromatography on a silica gel column using CH_2Cl_2 as eluent to give a yellow solid. Yield: 70% (0.44 g). ESI-MS (CH_2Cl_2): m/z 376.0 ($[M+H]^+$). IR (KBr): 3342, 3248, 1687, 1159, 769 cm^{-1}. ^1H NMR ($CDCl_3$, 400 MHz, TMS, ppm): δ 4.33 (S, 2H), 7.12 (t, J = 7.72 Hz, 1H), 7.43 (m, 3H), 7.51 (m, 1H), 7.83 (d, J = 7.44 Hz, 1H), 7.95 (d, J = 8.00 Hz, 1H), 8.10 (d, J = 8.23 Hz, 2H), 8.72 (m, 1H), 9.36 (s, 1H), 10.15 (s, 1H). ^{13}C NMR ($CDCl_3$, 400 MHz, ppm): δ 43.09 (chloroacetyl), 116.74 (quinoline), 122.14 (quinoline), 123.35 (quinoline), 123.63 (phenyl), 124.48 (phenyl), 126.69 (phenyl), 127.75 (quinoline), 128.24 (quinoline), 129.91 (phenyl), 132.75 (phenyl), 134.20 (quinoline), 134.73 (phenyl), 136.53 (quinoline), 138.78 (quinoline), 148.91 (quinoline), 164.70 (chloroacetyl).

1-(2-*N*-quinolin-8-yl-benzenesulfonamino-acetamide)-4,7,10-tris(*tert*-butoxy-carbonyl-methyl)-1,4,7,10-tetraaza-cyclododecane (3). A mixture of tris-*tert*-butyl-DO3A (0.26 g, 0.5 mmol), **2** (0.21 g, 0.56 mmol), and K_2CO_3 (0.5 g) in CH_3CN (40 mL) was stirred at 70 °C for 1 d. After cooling, the mixture was filtered, and the filtrate was evaporated to generate the crude residue, which was purified by chromatography on a silica gel column using CH_2Cl_2/CH_3OH (v/v = 20: 1) as eluent to give a light olive brown oil. Yield: 53% (0.23 g). ESI-MS (CH_2Cl_2): m/z 854.7 ($[M+H]^+$).^1H NMR ($CDCl_3$, 400 MHz, TMS, ppm): δ 1.42 (S, 18H), 1.47 (S, 9H), 2.80−3.50 (m, 24H), 7.06 (t, J = 7.68 Hz, 1H), 7.43 (m, 4H), 7.80 (d, J = 7.24 Hz, 1H), 7.90 (s, 1H), 8.07 (d, J = 8.28 Hz, 1H), 8.13 (s, 1H), 8.73 (s, 1H). ^{13}C NMR ($CDCl_3$, 400 MHz, ppm): δ 28.14 (methyl), 52.01, 52.57 (cyclene), 55.46 (acetamide), 56.66 (carbonyl-methyl), 77.25 (*tert*-butyl), 122.04 (quinoline), 122.98 (quinoline), 126.64 (phenyl and quinoline), 128.23 (phenyl), 129.84 (quinoline and phenyl), 133.21 (quinoline), 133.90 (phenyl), 135.47 (quinoline), 136.30 (quinoline and phenyl), 139.01 (quinoline), 148.94 (quinoline), 170.42 (carbonyl).

1-(2-*N*-quinolin-8-yl-benzenesulfonamino-acetamide)-4,7,10-tris(aceticacid)-1,4,7,10-tetraaza-cyclododecane (H_3L). To a CH_2Cl_2 (5 mL) solution of **3** (0.15 g, 0.14 mmol) was added trifluoroacetic acid (5 mL) with stirring. After stirring at ambient temperature for 1 d, the solution was evaporated, and the residue redissolved in CH_3OH. To the solution was added dropwise cold diethyl ether to precipitate the product as a white solid, which was filtered and dried in vacuo. Yield: 92% (0.11 g). ESI-MS (CH_3OH): m/z 686.7 ($[M+H]^+$). ^1H NMR (D_2O, 400 MHz, ppm): δ 2.80−3.90 (m, 24H), 6.96 (t, J = 7.64 Hz, 1H), 7.22 (d, J = 7.72 Hz, 1H), 7.44 (t, J = 8.26 Hz, 1H), 7.53 (t, J = 9.00 Hz, 2H), 7.60 (t, J = 15.69 Hz, 1H), 7.80 (m, 1H), 7.91 (d, J = 8.26 Hz, 1H), 8.77(d, J = 8.26, 1H), 8.92 (d, J = 4.16 Hz, 1H). ^{13}C NMR (D_2O, 400 MHz, ppm): δ 48.22, 51.49 (tetraazacyclododecane), 54.67 (acetamide), 56.49 (acetic acid), 122.08 (quinoline), 126.23 (quinoline), 127.54 (quinoline), 127.86 (phenyl), 128.39 (phenyl), 129.41 (phenyl), 129.48 (quinoline), 129.79 (quinoline), 129.99 (phenyl), 131.79 (phenyl), 134.02 (quinoline), 134.75 (phenyl), 136.09 (quinoline), 145.43 (quinoline), 146.38 (quinoline), 170.32 (acetamide), 173.64 (carboxyl).

GdL Complex. To an aqueous solution of H_3L (0.082 g, 0.12 mmol) was added dropwise 1 M NaOH solution until pH = 7.0. An equimolar amount of an aqueous solution of $GdCl_3{\cdot}6H_2O$ was slowly added. To maintain the pH at 7.0, 1 M NaOH solution was further added. Upon stirring at room temperature for 1 d, the solution was evaporated. The crude product was dissolved in a minimal volume of water, and acetone was added carefully to precipitate the product as a white solid. Yield: 87% (0.085 g). ESI-MS (CH_3OH): m/z 839.3 ($[M-H]^-$). Anal. Calcd for $GdL(H_2O){\cdot}6H_2O$: C, 38.54, H, 5.22, N, 10.15, Gd 16.28%. Found: C, 38.34, H, 4.91, N, 10.03, Gd 16.77%.

DyL Complex. This complex was prepared by the same synthetic procedure as that of the GdL complex. ESI-MS (CH_3OH): m/z 845.2 ($[M-H]^-$).

Physical Measurements. The ^1H and ^{13}C NMR spectra and ^{17}O NMR dysprosium induced shift (DIS) experiments were recorded at 400 MHz on a Bruker Avance III NMR spectrometer. Gadolinium content was determined on an Ultima 2 inductively coupled plasma OES (ICP-OES) spectrophotometer. Elemental analyses (C, H, and N) were carried out on a Perkin-Elemer model 240C elemental analyzer. ESI-MS were performed on a Finnigan LCQ mass spectrometer. Fourier transform infrared spectra were recorded on a Magna 750 FT-IR spectrophotometer with KBr pellet. Emission and excitation spectra were recorded on a Perkin-Elmer LS55 luminescence spectrometer with a red-sensitive photomultiplier type R928. UV−vis absorption spectra were measured on a Perkin−Elmer Lambda 25 UV−vis spectrometer. All of the spectra were recorded at 25 °C in a 100 mM HEPES buffer solutions at pH = 7.2.

Crystal Structural Determination. Crystals of $GdLZn(H_2O){\cdot}5H_2O$ suitable for X-ray diffraction studies were grown using a concentrated aqueous solution of GdL with equal amount of $ZnCl_2$ at pH = 7.0 through slow evaporation at ambient temperature. Data collection was performed on a SATURN70 CCD diffractometer by the ω scan technique at room temperature using graphite-monochromated Mo−Kα (λ = 0.71073 Å) radiation. The Crystal Clear software package was used for data reduction and empirical absorption correction. The structures were solved by direct methods. The heavy atoms were located from the E-map, and the rest of the non-hydrogen atoms were found in subsequent Fourier maps. All non-hydrogen atoms were refined anisotropically, while the hydrogen atoms were generated geometrically and refined with isotropic thermal parameters. The structures were refined on F^2 by full-matrix least-squares methods using the SHELXTL-97 program package.[19] The crystallographic data are summarized in Table 1.

Table 1. Crystallographic Data of $GdLZn(H_2O)_3{\cdot}5H_2O$

empirical formula	$C_{31}H_{50}GdN_7O_{17}SZn$
formula weight	1047.46
crystal System	triclinic
space group	$P\bar{1}$
a, Å	11.156(0)
b, Å	12.17940(10)
c, Å	17.03590(10)
α, deg	70.941(6)
β, deg	76.769(6)
γ, deg	64.777(5)
V, Å^3	1968.32(8)
Z	2
ρ_{calcd} g/cm^{-3}	1.767
μ, mm^{-1}	2.415
radiation (λ,Å)	0.71073
temp, (K)	293(2)
R1(F_o)^a	0.0336
wR2(F_o^2)^b	0.0827
GOF	1.066

$^a R1 = \sum||F_o| - |F_c||/\sum|F_o|$. $^b wR2 = \sum w(F_o^2 - F_c^2)^2/\sum w(F_o^2)]^{1/2}$.

T_1 Measurements. The longitudinal relaxation times (T_1) of aqueous buffer solutions of GdL were measured by a standard inversion−recovery pulse sequence on a PQ-001 NMR Analyzing & Imaging system (Shanghai Niumag Corporation) at 0.5 T. In each case, five samples were prepared separately whose concentrations were 0, 0.5, 1.0, 1.5, 2.0 mM Gd^{3+} at 25 °C in a 100 mM HEPES buffer solutions at pH = 7.2. The relaxivity r_1 is commonly used to express the ability of proton relaxation enhancement of a paramagnetic compound. It is defined as the slope of eq 1 with mM^{-1} s^{-1} as the unit.

$$(1/T_1)_{obs} = (1/T_1)_d + r_1[M] \quad (1)$$

dx.doi.org/10.1021/ic301308z | Inorg. Chem. 2012, 51, 9508−9516

where $(1/T_1)_{obs}$ and $(1/T_1)_d$ are the observed values in the presence and absence of the paramagnetic species, and [M] is the concentration of the paramagnetic species.

T_1-Weighted MRI Phantom Images. Phantom images were obtained using a MiniMR-60 NMR Analyzing & Imaging system (Shanghai Niumag Corporation). The instrumental parameters were set as 0.5 T magnet, section thickness = 60 mm, TE = 1.4 s, and TR = 5 ms.

^{17}O Dysprosium Induced Shift (DIS) Experiments. DIS experiments were performed on a 400 MHz Bruker Avance III NMR spectrometer. Dy^{3+} was used to be the analogue of DyL and $(DyL)_2Zn$. DIS measurements were performed in 100 mM HEPES buffer solutions containing 20% D_2O at pH = 7.2. DIS values were determined by plotting [Dy] versus −Δppm and calculating the slope of the resulting line. The calculated slopes were referenced to the slope obtained for $DyCl_3$ (q = 9).

Cell Culture. A human breast cancer cell line MDA-MB-231 was purchased from the Shanghai Institute of Cell Biology, Chinese Academy of Sciences, China. Cells were maintained in Dulbecco's modified Eagle's medium (DMEM) supplemented with 10% FBS (Fetal Bovine Serum) and antibiotics at 37 °C in a humidified incubator with 5% CO_2 atmosphere. The viability of cells was determined by Trypan blue dye exclusion. Cells were maintained in logarithmic phase with viability >95%.

Microscopy and Imaging Methods. The cells were mounted for direct microscopic observation at 37 °C. The confocal fluorescence images of cells were performed with an Olympus Fluo View FV1000 laser-scanning microscope. A 60× oil-immersion objective lens was used. Excitation was carried out with a semiconductor laser at λ = 360 nm, and the emission was collected in the range λ = 520 ± 50 nm, including the maximum emission wavelength of GdL (496 nm), $(GdL)_2Zn$ (503 nm), and GdLZn (530 nm). A total of 30 × 10^4 MDA-MB-231 cells were planted in confocal chamber slides (NEST) in the presence of medium for 1 d at 37 °C. After being washed three times with PBS buffer solution, the cells were treated with a PBS buffer solution of GdL (20 μM) for dye loading for 30 min at 37 °C; then the cells were incubated with a PBS solution of $ZnCl_2$ (30 μM) for 20 min at 37 °C. The stained cells were washed three times with PBS buffer. Then the treated cells were imaged by fluorescence microscopy. For the control experiment, cells were incubated with a PBS solution of GdL (20 μM) for dye loading for 30 min at 37 °C and washed three times with PBS buffer, then imaged by fluorescence microscopy.

■ ASSOCIATED CONTENT

Ⓢ Supporting Information

Figures giving additional UV−vis and emission spectra and X-ray crystallographic file in CIF format for the structure determination of compoundGdLZn$(H_2O)\cdot 5H_2O$. This material is available free of charge via the Internet at http://pubs.acs.org.

■ AUTHOR INFORMATION

Corresponding Author

*E-mail: czn@fjirsm.ac.cn.

Notes

The authors declare no competing financial interest.

■ ACKNOWLEDGMENTS

We thankfully acknowledge the financial support from the NSFC (20931006, U0934003, and 91122006), the 973 project (2007CB815304) from MSTC, and the NSF of Fujian Province (2011J01065).

■ REFERENCES

(1) (a) Zhou, J.; Liu, Z.; Li, F. Y. *Chem. Soc. Rev.* **2012**, *41*, 1323−1349. (b) Jennings, L. E.; Long, N. J. *Chem. Commun.* **2009**, 3511−3524. (c) Ke, H. T.; Wang, J. R.; Dai, Z. F.; Jin, Y. S.; Qu, E. Z.; Xing, Z. W.; Guo, C. X.; Yue, X. L.; Liu, J. B. *Angew. Chem., Int. Ed.* **2011**, *50*, 3017−3021. (d) Ke, H. T.; Wang, J. R.; Dai, Z. F.; Jin, Y. S.; Qu, E. Z.; Xing, Z. W.; Guo, C. X.; Liu, J. B.; Yue, X. L. *J. Mater. Chem.* **2011**, *21*, 5561−5564.

(2) (a) Zhao, Q.; Li, F. Y.; Huang, C. H. *Chem. Soc. Rev.* **2010**, *39*, 3007−3030. (b) Koullourou, T.; Natrajan, L. S.; Bhavsar, H.; Pope, S. J. A.; Feng, J. H.; Narvainen, J.; Shaw, R.; Scales, E.; Kauppinen, R.; Kenwright, A. M.; Faulkner, S. *J. Am. Chem. Soc.* **2008**, *130*, 2178−2179. (c) Meng, Q. T.; Zhang, X. L.; He, C.; He, G. J.; Zhou, P.; Duan, C. Y. *Adv. Funct. Mater.* **2010**, *20*, 1903−1909.

(3) (a) Lauffer, R. B. *Chem. Rev.* **1987**, *87*, 901−927. (b) Caravan, P.; Ellison, J. J.; McMurry, T. J.; Lauffer, R. B. *Chem. Rev.* **1999**, *99*, 2293−2352. (c) Werner, E. J.; Datta, A.; Jocher, C. J.; Raymond, K. N. *Angew. Chem., Int. Ed.* **2008**, *47*, 8568−8580. (d) Woods, M.; Woessner, D. E.; Sherry, A. D. *Chem. Soc. Rev.* **2006**, *35*, 500−511. (e) Moats, R. A.; Fraser, S. E.; Meade, T. J. *Angew. Chem., Int. Ed.* **1997**, *36*, 726−728.

(4) (a) Mishra, A.; Pfeuffer, J.; Mishra, R.; Engelmann, J.; Mishra, A. K.; Ugurbil, K.; Logothetis, N. K. *Bioconjugate Chem.* **2006**, *17*, 773−780. (b) Hueber, M.; Staubli, A. B.; Kustedjo, K.; Gray, M. H. B.; Shih, J.; Fraser, S. E.; Jacobs, R. E.; Meade, T. J. *Bioconjugate Chem.* **1998**, *9*, 242−249. (c) Tu, C. Q.; Louie, A. Y. *Chem. Commun.* **2007**, 1331−1333. (d) Guo, K.; Berezin, M. Y.; Zheng, J.; Akers, W.; Lin, F.; Teng, B.; Vasalatiy, O.; Gandjbakhche, A.; Griffiths, G. L.; Achilefu, S. *Chem. Commun.* **2010**, *46*, 3705−3707. (e) Mamedov, I.; Engelmann, J.; Eschenko, O.; Beyerleina, M.; Logothetis, N. K. *Chem. Commun.* **2012**, *48*, 2755−2757. (f) Wang, B. D.; Hai, J.; Wang, Q.; Li, T. R.; Yang, Z. Y. *Angew. Chem., Int. Ed.* **2011**, *123*, 3119−3122. (g) Xi, P. X.; Cheng, K.; Sun, X. L.; Zeng, Z. Z.; Sun, S. H. *Chem. Commun.* **2012**, *48*, 2952−2954. (h) Kotková, Z.; Kotek, J.; Jirák, D.; Jendelová, P.; Herynek, V.; Berková, Z.; Hermann, P.; Lukes, I. *Chem.—Eur. J.* **2010**, *16*, 10094−10102.

(5) (a) Quea, E. L.; Chang, C. J. *Chem. Soc. Rev.* **2010**, *39*, 51−60. (b) Hanaoka, K.; Kikuchi, K.; Urano, Y.; Nagano, T. *J. Chem. Soc., Perkin Trans. 2* **2001**, 1840−1843. (c) Major, J. L.; Boiteau, R. M.; Meade, T. J. *Inorg. Chem.* **2008**, *47*, 10788−10795. (d) Li, W. H.; Parigi, G.; Fragai, M.; Luchinat, C.; Meade, T. J. *Inog. Chem* **2002**, *41*, 4018−4024. (e) Esqueda, A. C.; Lopez, J. A.; Andreu-de-Riquer, G.; Alvarado-Monzon, J. C.; Ratnakar, J.; Lubag, A. J. M.; Sherry, A. D.; De Leon-Rodrıguez, L. M. *J. Am. Chem. Soc.* **2009**, *131*, 11387−11391. (f) Que, E. L.; Chang, C. J. *J. Am. Chem. Soc.* **2006**, *128*, 15942−15943. (g) Li, W, S.; Luo, J.; Chen, Z. N. *Dalton Trans.* **2011**, *40*, 484−488. (h) Trokowski, R.; Ren, J.; Kálmán, F. K.; Sherry, A. D. *Angew. Chem., Int. Ed.* **2005**, *44*, 6920−6923. (i) Surman, A. J.; Bonnet, C. S.; Lowe, M. P.; Kenny, G. D.; Bell, J. D.; Tóth, É.; Vilar, R. *Chem.—Eur. J.* **2011**, *17*, 223−230.

(6) Zhang, X. L.; Jing, X.; Liu, T.; Han, G.; Li, H. Q.; Duan, C. Y. *Inorg. Chem.* **2012**, *51*, 2325−2331.

(7) (a) Solomon, I. *Phys. Rev.* **1955**, *99*, 559−565. (b) Bloembergen, N. *J. Chem. Phys.* **1957**, *27*, 572−573. (c) Bloembergen, N.; Morgan, L. O. *J. Chem. Phys.* **1961**, *34*, 842−850.

(8) Britton, M. M. *Chem. Soc. Rev.* **2010**, *39*, 4036−4043.

(9) (a) Fahrni, C. J.; O'Halloran, T. V. *J. Am. Chem. Soc.* **1999**, *121*, 11448−11458. (b) Pearce, D. A.; Jotterand, N.; Carrico, I. S.; Imperiali, B. *J. Am. Chem. Soc.* **2001**, *123*, 5160−5161. (c) Rouffet, M.; de Oliveira, C. A. F.; Udi, Y.; Agrawal, A.; Sagi, I.; McCammon, J. A.; Cohen, S. M. *J. Am. Chem. Soc.* **2010**, *132*, 8232−8233. (d) Jiang, P. J.; Guo, Z. J. *Coord. Chem. Rev.* **2004**, *248*, 205−229.

(10) Livramento, J. B.; Weidensteiner, C.; Prata, M. I. M.; Allegrini, P. R.; Geraldes, C. F. G. C.; Helm, L.; Kneuer, R.; Merbach, A. E.; Santos, A. C.; Schmidt, P.; Tóth, É. *Contrast Media Mol. Imaging* **2006**, *1*, 30−39.

(11) (a) Faller, P.; Hureau, C. *Dalton Trans.* **2009**, 1080−1094. (b) Smith, D. G.; Cappai, R.; Barnham, K. J. *Biochim. Biophy. Acta* **2007**, *1768*, 1976−1990.

(12) Giardiello, M.; Lowe, M. P.; Botta, M. *Chem. Commun.* **2007**, 4044−4046.

(13) Que, E. L.; Gianolio, E.; Baker, S. L.; Aime, S.; Chang, C. J. *Dalton Trans.* **2010**, *39*, 469−476.

(14) Dubost, J. P.; Leger, J. M.; Langlois, M. H.; Meyer, D.; Schaefer, M. *C. R. Acad. Sci., Ser. II Univers.* **1991**, *312*, 349−354.

(15) Alpoim, M. C.; Urbano, A. M.; Geraldes, C.; Peters, J. A. *J. Chem. Soc., Dalton Trans.* **1992**, 463−467.
(16) (a) Costa, J.; Ruloff, R.; Burai, L.; Helm, L.; Merbach, A. E. *J. Am. Chem. Soc.* **2005**, *127*, 5147−5157. (b) Livramento, J. B.; Toth, É.; Sour, A.; Borel, A.; Merbach, A. E.; Ruloff, R. *Angew. Chem., Int. Ed.* **2005**, *44*, 1480−1484. (c) Song, Y.; Kohlmeir, E. K.; Meade, T. J. *J. Am. Chem. Soc.* **2008**, *130*, 6662−6663. (d) Nicolle, G. M.; Tóth, E.; Schmitt-Willich, H.; Radüchel, B.; Merbach, A. E. *Chem.—Eur. J.* **2002**, *8*, 1040−1048. (e) Livramento, J. B.; Sour, A.; Borel, A.; Merbach, A. E.; Tóth, É. *Chem.—Eur. J.* **2006**, *12*, 989−1003.
(17) Xie, Y. L.; Gong, G. L.; Liu, Y. D.; Deng, S. X.; Rinderspacher, A.; Branden, L.; Landry, D. W. *Tetrahedron Lett.* **2008**, *49*, 2320−2323.
(18) Prasuhn, D. E.; Yeh, R. M.; Obenaus, A.; Manchester, M.; Finn, M. G. *Chem. Commun.* **2007**, 1269−1271.
(19) Sheldrick, G. M. *SHELXL-97, Program for the Refinement of Crystal Structures*; University of Göttingen: Göttingen, Germany, 1997.